PNAS RESEARCH ARTICLE | IMMUNOLOGY AND INFLAMMATION

Maternal IL-33 critically regulates tissue remodeling and type 2 immune responses in the uterus during early pregnancy in mice

Nuriban Valero-Pacheco[a,b], Eric K. Tang[a,b], Noura Massri[c,d,e], Rachel Loia[f,g], Anat Chemerinski[g], Tracy Wu[g], Salma Begum[g], Darine W. El-Naccache[a,f,h], William C. Gause[a,h], Ripla Arora[c,d], Nataki C. Douglas[a,g,1], and Aimee M. Beaulieu[a,b,1,2]

Edited by Thomas Spencer, University of Missouri, Columbia, MO; received December 23, 2021; accepted July 16, 2022

The pregnant uterus is an immunologically rich organ, with dynamic changes in the inflammatory milieu and immune cell function underlying key stages of pregnancy. Recent studies have implicated dysregulated expression of the interleukin-1 (IL-1) family cytokine, IL-33, and its receptor, ST2, in poor pregnancy outcomes in women, including recurrent pregnancy loss, preeclampsia, and preterm labor. How IL-33 supports pregnancy progression in vivo is not well understood. Here, we demonstrate that maternal IL-33 signaling critically regulates uterine tissue remodeling and immune cell function during early pregnancy in mice. IL-33–deficient dams exhibit defects in implantation chamber formation and decidualization, and abnormal vascular remodeling during early pregnancy. These defects coincide with delays in early embryogenesis, increased resorptions, and impaired fetal and placental growth by late pregnancy. At a cellular level, myometrial fibroblasts, and decidual endothelial and stromal cells, are the main IL-33$^+$ cell types in the uterus during decidualization and early placentation, whereas ST2 is expressed by uterine immune populations associated with type 2 immune responses, including ILC2s, Tregs, CD4$^+$ T cells, M2- and cDC2-like myeloid cells, and mast cells. Early pregnancy defects in IL-33–deficient dams are associated with impaired type 2 cytokine responses by uterine lymphocytes and fewer Arginase-1$^+$ macrophages in the uterine microenvironment. Collectively, our data highlight a regulatory network, involving crosstalk between IL-33–producing nonimmune cells and ST2$^+$ immune cells at the maternal–fetal interface, that critically supports pregnancy progression in mice. This work has the potential to advance our understanding of how IL-33 signaling may support optimal pregnancy outcomes in women.

IL-33 | pregnancy | type 2 immunity | tissue remodeling | decidual vasculature

Complex and dynamic inflammatory processes underlie the sequential progression of mammalian pregnancy from blastocyst implantation through labor. These inflammatory processes are orchestrated in part by the many subsets of maternal immune cells that reside at or are recruited to the maternal–fetal interface throughout pregnancy. Previous work has revealed that these immune cells produce and respond to cytokines, growth factors, immunoregulatory molecules, and other mediators that regulate diverse aspects of pregnancy, ranging from tissue and vascular remodeling to fetal tolerance (1–3). Despite these advances, our understanding of how these immunological mediators support distinct stages of pregnancy remains poorly defined. Given that abnormal inflammatory and immune responses are associated with many pregnancy disorders, it is critical that we address these knowledge gaps to develop new therapeutic interventions that promote successful pregnancy outcomes (1–3).

Recent studies have highlighted an intriguing, but still poorly understood, link between the interleukin-1 (IL-1) family cytokine, interleukin-33 (IL-33), and pregnancy-related disorders in women. Genome-wide association studies (GWAS) have identified single-nucleotide polymorphisms (SNPs) in the *IL33* gene that are associated with recurrent or idiopathic pregnancy loss (4–6). Other groups have reported abnormal levels of IL-33 or ST2 in serum or uterine tissue from women with preeclampsia (7–11), placenta previa accreta (12), gestational diabetes mellitus (13), and recurrent or impending pregnancy loss (14, 15). Notably, both reduced and excessive IL-33 expression have been observed in distinct pregnancy disorders, suggesting that the magnitude and/or timing of IL-33 signaling may be a critical determinant of its specific biological effects on pregnancy outcomes (4, 5, 7, 10–13, 15, 16). Nevertheless, few studies have addressed the functional requirement for IL-33 during pregnancy progression in vivo, and these have principally focused on very late gestation in lipopolysaccharide

Significance

Recent clinical studies suggest that abnormal interleukin-33 (IL-33) signaling is associated with poor pregnancy outcomes in women, including recurrent pregnancy loss, preeclampsia, and preterm labor. Nevertheless, how IL-33 supports pregnancy progression in mammals is not well understood. Here, we show that pregnant mice lacking the *Il33* gene exhibit a broad spectrum of cellular, physiological, and immunological defects that manifest very early in pregnancy. Our data suggest that IL-33 signaling supports diverse, pro-pregnancy processes at the maternal–fetal interface during early gestation, which in turn lay the foundation for optimal outcomes at later stages of pregnancy. Ultimately, our findings have the potential to inform therapeutic applications and interventions that target IL-33 to improve pregnancy outcomes in women.

Author contributions: N.V.-P., W.C.G., R.A., N.C.D., and A.M.B. designed research; N.V.-P., E.K.T., N.M., R.L., A.C., T.W., S.B., D.W.E.-N., R.A., N.C.D., and A.M.B. performed research; W.C.G. contributed new reagents/analytic tools; N.V.-P., E.K.T., N.M., R.L., A.C., T.W., S.B., D.W.E.-N., R.A., N.C.D., and A.M.B. analyzed data; and N.V.-P. and A.M.B. wrote the paper.

The authors declare no competing interest.

This article is a PNAS Direct Submission.

[1]N.C.D. and A.M.B. contributed equally to this work.

[2]To whom correspondence may be addressed. Email: ab1550@njms.rutgers.edu.

This article contains supporting information online at http://www.pnas.org/lookup/suppl/doi:10.1073/pnas.2123267119/-/DCSupplemental.

Published August 22, 2022.

(LPS)-challenged mice (17, 18). Collectively, these data suggest that properly regulated IL-33 signaling may be an important feature of mammalian pregnancy and highlight the need to better understand the contributions of IL-33 to the physiological and cellular processes that underlie a healthy pregnancy.

IL-33 is an unusual cytokine with pleiotropic effects on host immunity in diverse tissues and inflammatory environments (19–21). IL-33 is widely described as an alarmin that functions as a nuclear protein in healthy cells but is released as a cytokine into the extracellular milieu in response to inflammation, tissue damage, or cell death (19–21). Its expression has been reported in a variety of "structural" cell types—e.g., epithelial, stromal, fibroblast, myofibroblast, and endothelial cells—depending on the tissue and inflammatory condition, although immune cells may also produce IL-33 in certain settings (19, 20). IL-33 signals through a heterodimeric receptor composed of an IL-33–specific subunit, ST2, and the shared IL-1 receptor accessory protein (IL-1RAcP) (19–21). ST2 is typically, but not exclusively, expressed on immune cells associated with type 2 inflammatory and tissue repair responses, such as group 2 innate lymphoid cells (ILC2s), type 2 helper $CD4^+$ T cells (Th2), $CD4^+$ regulatory T cells (Tregs), subsets of dendritic cells (e.g., cDC2s), M2-polarized macrophages, and mast cells (20, 21). Consistent with this expression pattern, IL-33 signaling has well-established roles in type 2 immune responses associated with both host defense and tissue remodeling in a wide variety of tissues and disease states, including allergy, sterile inflammation, helminth infection, fibrosis, and wound healing (19, 20, 22).

Early pregnancy progression depends on extensive remodeling of the endometrial tissue and vasculature to facilitate nutrient and waste exchange with the developing embryo prior to formation of the definitive placenta. In mice, blastocyst implantation on embryonic day (E) 4.5 of pregnancy results in formation of the implantation chamber and triggers a process known as decidualization, during which endometrial cells differentiate into highly specialized decidual stromal cells and vascular networks rapidly expand to support the developing embryo (23, 24). Defects in tissue and vascular remodeling during early pregnancy can have adverse "ripple effects" on placental formation and function at later stages of pregnancy, contributing to a broad range of pregnancy disorders, including preeclampsia, fetal growth restriction, preterm labor, and even overt pregnancy loss (25). How IL-33 signaling impacts these early, foundational processes in vivo is poorly understood.

Here, we demonstrate that maternal IL-33 critically regulates the physiological and immunological processes that support uterine remodeling and embryo development during early pregnancy in mice. IL-33–deficient dams exhibit defects in implantation chamber formation, uterine decidualization, and vascular remodeling in the post-implantation phase of early pregnancy, prior to formation of the placenta. These defects coincide with significant delays in early embryo development, increased pregnancy resorptions, and defects in fetal and placental growth by late gestation. Our data suggest that IL-33–mediated crosstalk between non-immune and immune cells in the pregnant uterus underlies healthy pregnancy progression in mice, and we find that the pregnancy defects in IL-33–deficient dams are associated with impaired immune responses by type 2 immune cells at the maternal–fetal interface during early pregnancy. Altogether, our data provide important mechanistic insights into the functional role of IL-33 signaling in pregnancy progression in mammals.

Results

Myometrial Fibroblasts and Decidual Stromal and Endothelial Cells Are the Principal IL-33–Expressing Cell Types in the Uterus during the Post-Implantation Phase of Early Pregnancy. IL-33 can be produced by diverse cell types depending on the tissue and immunological setting (20, 21). We therefore sought to identify IL-33–expressing cells in the uterus during early pregnancy. For these studies, wild-type (WT) studs were mated with IL-33 Citrine reporter females ($Il33^{cit/wt}$) (26) and $Citrine^+$ cells in the pregnant uterus were first evaluated by fluorescence microscopy at E7.5 and E9.5, time points that correspond to the peak of decidual angiogenesis and early placentation, respectively, in mice (23). These studies revealed numerous $Citrine^+$ cells in the myometrium, the muscle-rich layer of tissue encapsulating each implantation site, whereas $Citrine^+$ cells were present but less frequent in the decidua (Fig. 1*A* and *SI Appendix*, Fig. S1*A*). Among those in the decidua, many costained with the endothelial cell marker, $CD31^+$, and localized to the mesometrial pole (Fig. 1*A* and *SI Appendix*, Fig. S1 *A*, *Lower*). Kinetic studies using flow cytometry confirmed that ∼17 to 30% of total cells in the myometrium, but only ∼1 to 4% in the decidua, were $Citrine^+$ in the post-implantation phase of early pregnancy (Fig. 1 *B* and *C*). We further validated our data by performing Western blots on whole-tissue lysates from WT dams using an αIL-33 antibody, which showed that IL-33 protein was more abundant in the myometrium than the decidua at E7.5. However, the majority of IL-33 in the myometrium was present in its full-length, ∼30-kDa form, whereas both full-length and ∼20-kDa mature forms were present in the decidua (Fig. 1*D*) (27). These findings suggest that IL-33 may be more bioactive in the decidua than in the myometrium, as prior studies have shown that the mature forms of IL-33 are more potent than full-length forms of the protein (28, 29).

To better define the cellular identity of IL-33–expressing cells in the uterus during early pregnancy, we performed unbiased single-cell RNA sequencing (scRNA-seq) on sort-purified $Citrine^+$ cells isolated separately from the myometrium and decidua of pregnant $Il33^{cit/wt}$ dams at E7.5. Individual cells with detectable *Il33* transcripts were identified among the bulk dataset and further analyzed using unbiased clustering algorithms. These analyses revealed four distinct clusters of $Il33^+$ cells in the myometrium (Fig. 1*E*) and three distinct clusters in the decidua (Fig. 1*H*), highlighting a degree of heterogeneity among the $Il33^+$ cell populations in these tissue layers. Nevertheless, the large majority of $Il33^+$ cells in the myometrium (1,522 of 1,586 total cells) belonged to clusters 1 and 2, which expressed genes associated with fibroblast or stromal cells, including *Pdpn*, *Pdgfra*, *Pdgfrb*, *Col1a1*, *Fn1*, and *Ly6a* (Fig. 1*F* and *SI Appendix*, Fig. S2*A*) (30, 31). Cells in cluster 1 also expressed genes such as *Acta2*, *Klf5*, *Hic1*, and *Gli1* (Fig. 1*F* and *SI Appendix*, Fig. S2*A*), consistent with a myofibroblast identity (32, 33). Of the two minor non-fibroblast clusters, cluster 3 was composed of epithelial cells, identified based on high expression of multiple keratin genes and *Fgf9* (Fig. 1*F* and *SI Appendix*, Fig. S2*B*), and cluster 4 was composed of endothelial cells with high expression of vascular genes, such as *Pecam1*, *Plvap*, *Cdh5*, *Icam2*, *Ptprb*, *Selp*, and *Nos3* (Fig. 1*F* and *SI Appendix*, Fig. S2*C*). Kinetic studies performed by flow cytometry at E5.5, E7.5, and E9.5 validated our scRNA-seq data and demonstrated that >80% of $Citrine^+$ cells in the myometrium expressed the fibroblast/stromal cell marker, Podoplanin (encoded by *Pdpn*), whereas only minor populations of $CD31^+CD45^-$ $Podoplanin^-$ endothelial cells and $Epcam^+CD45^-$ epithelial cells were present at all three time points (Fig. 1*G*).

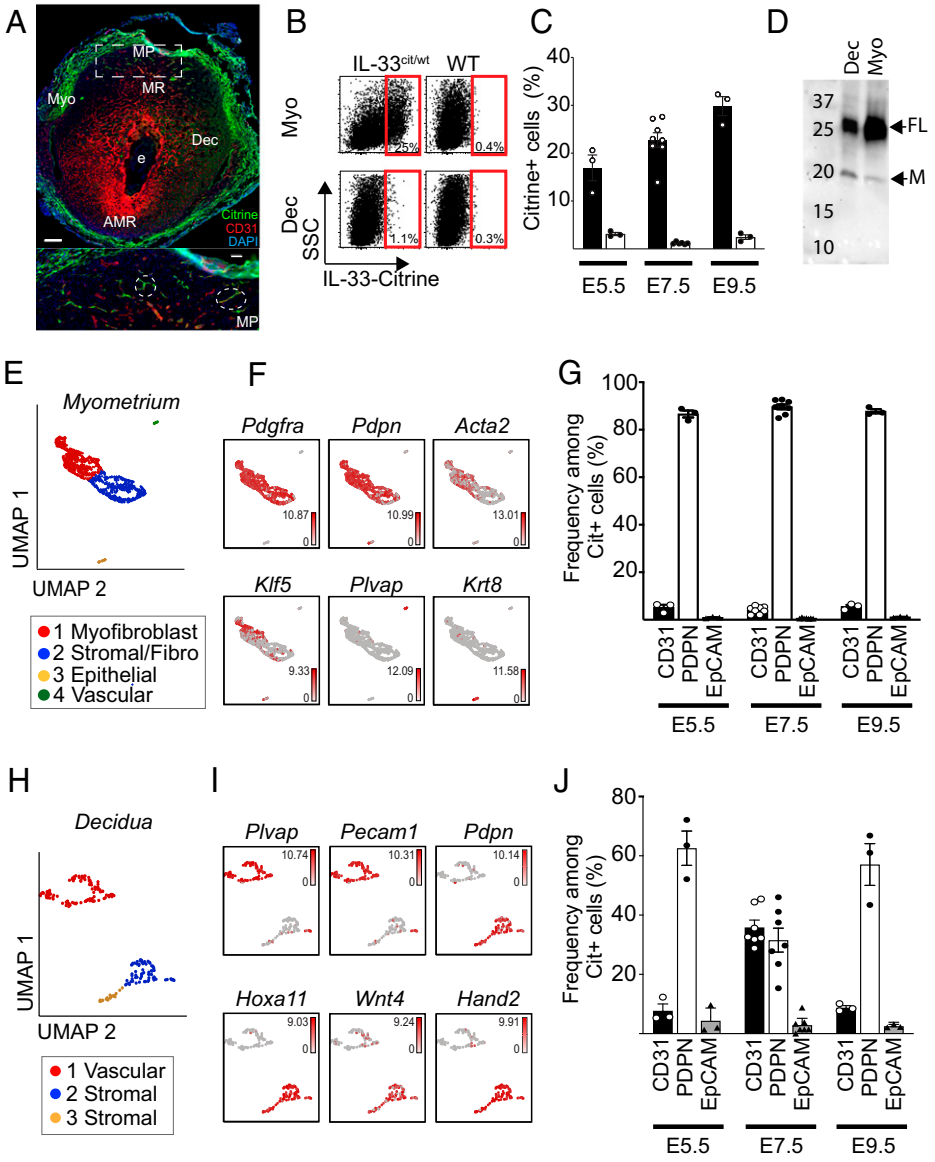

Fig. 1. Myometrial fibroblasts and decidual stromal and endothelial cells are the main IL-33$^+$ cell types in the uterus in early pregnancy. (*A*) Image (20×) (*Top*) showing Citrine, CD31, and DAPI in an implantation site (IS) from an IL-33 Citrine fluorescent reporter dam at E7.5; the rectangle denotes the mesometrial pole region shown as a 40× image (*Bottom*) with Citrine$^+$CD31$^+$ vessels in white ellipses. (Scale bars, 200 μm [*Top*] and 50 μm [*Bottom*].) AMR, antimesometrial region; Dec, decidua; e, embryo; MP, mesometrial pole; MR, mesometrial region; Myo, myometrium. Representative of $n = 3$ dams, 2 or 3 ISs per dam. (*B* and *C*) Dot plots at E7.5 (*B*) and summary data (*C*) showing the percentage of Citrine$^+$ cells among total live cells in the Myo (open circles, black bars) and Dec (closed circles, white bars) of ISs from IL-33 Citrine fluorescent reporter dams at E5.5, E7.5, and E9.5 ($n = 3$ to 8 dams, 7 to 11 pooled ISs per dam) by flow cytometry. *B* includes a dot plot of cells from WT nonreporter dams at E7.5, used to determine gates for Citrine$^+$ cells. (*D*) Western blot of IL-33 in the Myo and Dec from ISs from a WT dam at E7.5. Representative of $n = 3$ dams, 3 pooled ISs per dam. FL, full-length form; M, mature form. (*E*, *F*, *H*, and *I*) Live Citrine$^+$ cells in the Myo and Dec ($n = 9$ pooled ISs) at E7.5 were analyzed by scRNA-seq. Cells with detectable *Il33* transcripts were selected and clustered by *K*-means clustering. (*E* and *H*) Uniform manifold approximation and projection (UMAP) shows unbiased clustering of *Il33*$^+$ cells from Myo (*E*) or Dec (*H*). (*F* and *I*) Feature plots show expression of specified transcripts in individual *Il33*$^+$ cells from Myo (*F*) or Dec (*I*). (*G* and *J*) Percentage of Podoplanin$^+$ CD31$^-$EpCAM$^-$CD45$^-$, CD31$^+$CD45$^-$ cells, and EpCAM$^+$CD45$^-$ cells among live Citrine$^+$ cells in Myo (*G*) and Dec (*J*) at E5.5, E7.5, and E9.5 by flow cytometry ($n = 3$ to 8 dams, 7 to 11 pooled ISs per dam). Data points represent individual dams. Data are displayed as mean ± SEM.

Among the three clusters of *Il33*$^+$ cells identified in the decidua (Fig. 1*H*), cluster 1 contained cells with high expression of endothelial cell genes, including *Plvap* and *Pecam1* (Fig. 1*I* and *SI Appendix*, Fig. S2*D*). Clusters 2 and 3 contained cells with high expression of stromal cell or fibroblast genes (e.g., *Pdpn*, *Pdgfra*, *Col5a2*, and *Col1a1*), including many genes that are specifically associated with decidualized stromal cells such as *Hoxa11*, *Hand2*, *Wnt4*, *Fkbp5*, *Pgr*, and *Bmpr1a* (23) (Fig. 1*I* and *SI Appendix*, Fig. S2*E*). Cluster 3 also exhibited a pro-proliferative gene signature (34) (e.g., *Mki67*, *Ccna2*, *Aurka*, *Bub1a*, and *Top2a*), indicative of a proliferating decidual stromal cell subset (*SI Appendix*, Fig. S2*F*). Thus, most *Il33*$^+$ cells in the decidua exhibited gene signatures that were consistent with either an endothelial or decidual stromal cell identity. These findings were validated by flow cytometry, which demonstrated that ∼37% of IL-33$^+$ cells in the decidua were CD31$^+$CD45$^-$ endothelial cells at E7.5, although the relative frequency was significantly lower (<10%) at E5.5 and E9.5 (Fig. 1*J*). In contrast, the relative frequency of IL-33$^+$ cells that expressed the stromal cell marker, Podoplanin, was ∼30% at E7.5 but >50% at E5.5 and E9.5. Altogether, our data suggest that IL-33–expressing cells are abundant in the pregnant uterus, with myometrial stromal cells/fibroblasts and myofibroblasts representing the majority, and decidual endothelial cells and stromal cells representing

the minority, of IL-33$^+$ cells during the post-implantation phase of pregnancy, prior to formation of the definitive placenta.

Maternal IL-33 Deficiency Leads to Defects in Uterine Tissue Remodeling and Early Embryo Development. Given our finding that IL-33 is highly expressed in the uterus in early gestation, we next sought to determine the impact of maternal IL-33 deficiency on early pregnancy progression. Our initial studies revealed that the frequency of dams with a detectable pregnancy at E7.5, following a copulation plug at E0.5, was similar in WT dams and *Il33*$^{cit/cit}$ dams, which lack both copies of the *Il33* gene and are hereafter referred to as IL-33 knockout (KO) mice (*SI Appendix*, Fig. S3*A*). Additionally, the total number of implantation sites at E7.5 was only modestly (~16%) reduced in IL-33 KO dams relative to WT dams (*SI Appendix*, Fig. S3*B*), and this reduction did not reach statistical significance until large numbers of dams (>48 per group) were analyzed. Nevertheless, three-dimensional (3D) immunofluorescence imaging studies (35) revealed that implantation chambers were significantly smaller in IL-33 KO dams compared with WT dams at E5.5 (Fig. 2 *A* and *B*), a finding that mirrored smaller implantation sites in IL-33 KO versus WT dams at E7.5 (Fig. 2*C*). These observations suggested that uterine remodeling processes initiated in response to blastocyst implantation may be impaired. Consistent with this idea, genes associated with uterine decidualization, including *Wnt4* and *Fkbp5*, were expressed at significantly lower levels in whole-decidual tissue from IL-33 KO dams compared with WT dams, possibly reflecting a defect in the abundance and/or differentiation state of decidual stromal cells at E7.5 (Fig. 2*D*). Collectively, these data suggest that maternal IL-33 signaling plays important roles in the uterine remodeling and decidualization processes that are initiated by blastocyst implantation during early pregnancy in mice.

Because post-implantation uterine remodeling and decidualization are essential to support the embryo prior to formation of the placenta, we next evaluated the impact of maternal IL-33 deficiency on embryo development. Three-dimensional imaging analyses showed that embryos were smaller in IL-33 KO versus WT dams at E5.5 (Fig. 2 *E* and *F*). Moreover, when scored at E7.5 for morphologic features reflecting the consecutive primitive streak, neural plate, and headfold stages of gastrulation that occur between E6.5 and E8.5 in WT mice (36), more embryos from IL-33 KO dams were in the earlier primitive streak stage, and fewer were in the later neural plate stage, compared with embryos from WT dams (Fig. 2*G*). Consistent with a defect in early embryo development, the frequency of resorptions was significantly higher in IL-33 KO versus WT dams at day E12.5 (Fig. 2 *H* and *I*). Taken together, our data suggest that maternal IL-33 signaling critically regulates implantation chamber formation and uterine decidualization, and is required for optimal embryo development, during early pregnancy in mice.

IL-33 KO Dams Exhibit Abnormal Decidual Vascularization and Spiral Artery Remodeling during Early Pregnancy. Uterine decidualization is accompanied by a surge in angiogenesis and vascular remodeling, which serve to support the developing embryo and establish a foundation for the placental vasculature (37). Decidual angiogenesis, which occurs between E5.5 and E8.5 in mice, results in distinct types of blood vessels in the mesometrial and antimesometrial regions of the decidua. Newly formed capillaries are widely distributed throughout the decidua, while spiral arteries (SpAs), noted for their coverage with αSMA$^+$ vascular smooth muscle cells, are localized to the mesometrial pole (38, 39). SpAs undergo extensive remodeling during placentation from E8.5 to E12.5, ultimately transforming into the specialized high-volume blood vessels that connect the maternal and fetal circulatory systems in the placenta (40).

Given our findings that maternal IL-33 deficiency disrupts uterine decidualization and that IL-33 is expressed by decidual endothelial cells, we evaluated the effects of maternal IL-33 deficiency on decidual vascularization. We found that the density of decidual CD31$^+$ blood vessels in the mesometrial pole was higher in IL-33 KO dams relative to WT dams at E7.5, although this result was region-specific as neither the central nor anti-mesometrial regions of the implantation site exhibited IL-33–dependent changes in vessel density (Fig. 3 *A* and *B* and *SI Appendix*, Fig. S4*A*). The increase in vessel density at the mesometrial pole was not due to changes in the density of nascent SpAs, identified by expression of αSMA, because SpA density was similar in IL-33 KO and WT dams at E7.5 (Fig. 3*C* and *SI Appendix*, Fig. S4*B*). These data suggest that a denser capillary network at the mesometrial pole, which undergoes rapid expansion during decidualization, may explain the increased density of blood vessels observed in this region in IL-33 KO dams at E7.5. Nevertheless, investigation of SpA morphology at E9.5, when SpAs are actively enlarging and remodeling to support the developing placenta, revealed that SpAs in IL-33 KO dams had larger cross-sectional areas and thicker walls (Fig. 3 *D* and *E*). Taken together, our data suggest that IL-33 is critical for proper remodeling of the uterine vasculature during early pregnancy, with dual roles in restricting the extent of decidual angiogenesis in the mesometrial pole and promoting proper SpA architecture during early placentation.

Maternal IL-33 Deficiency Impairs Fetal and Placental Growth during Late Gestation. Abnormalities in uterine tissue and vascular remodeling during early pregnancy can negatively impact placental and fetal development at later stages of pregnancy, in some cases resulting in intrauterine growth restriction or overt pregnancy loss. We therefore assessed the impact of maternal IL-33 deficiency on pregnancy progression during late gestation in mice. Compared with WT dams, IL-33 KO dams harbored significantly fewer viable fetuses and significantly more fetal resorptions at E18.5 (Fig. 4 *A*–*C*). Moreover, compared with WT dams, viable fetuses in IL-33 KO dams were smaller and a higher frequency were identified as "small for gestational age" (SGA), with weights at or below the 10th percentile of WT fetuses from WT dams (Fig. 4 *D* and *E*). The increased incidence of poor pregnancy outcomes in IL-33 KO dams was accompanied by placental abnormalities that included significant reductions in placental diameter and labyrinth zone area, as compared with WT dams, although overall placental weights and fetal-to-placental weight ratios were comparable in WT and KO dams (Fig. 4*F* and *SI Appendix*, Fig. S5 *A*–*E*). Importantly, viable fetus numbers, fetal weights, placental diameter, and frequency of SGA fetuses were similar in WT dams mated with IL-33 KO or WT sires (Fig. 4 *B*, *D*, *E*, and *F*), suggesting that fetal *Il33* heterozygosity does not impair these readouts of pregnancy progression at E18.5. In summary, our data highlight a critical role for maternal IL-33 in supporting optimal pregnancy outcomes at both early and late stages of gestation in mice.

Immune Cells Associated with Type 2 Responses Express ST2 at the Maternal–Fetal Interface at E7.5. IL-33 is a pleiotropic cytokine with diverse roles in host immunity. In addition to its well-established role in type 2 immune responses, IL-33 has also been shown to act on immune cells associated with type 1

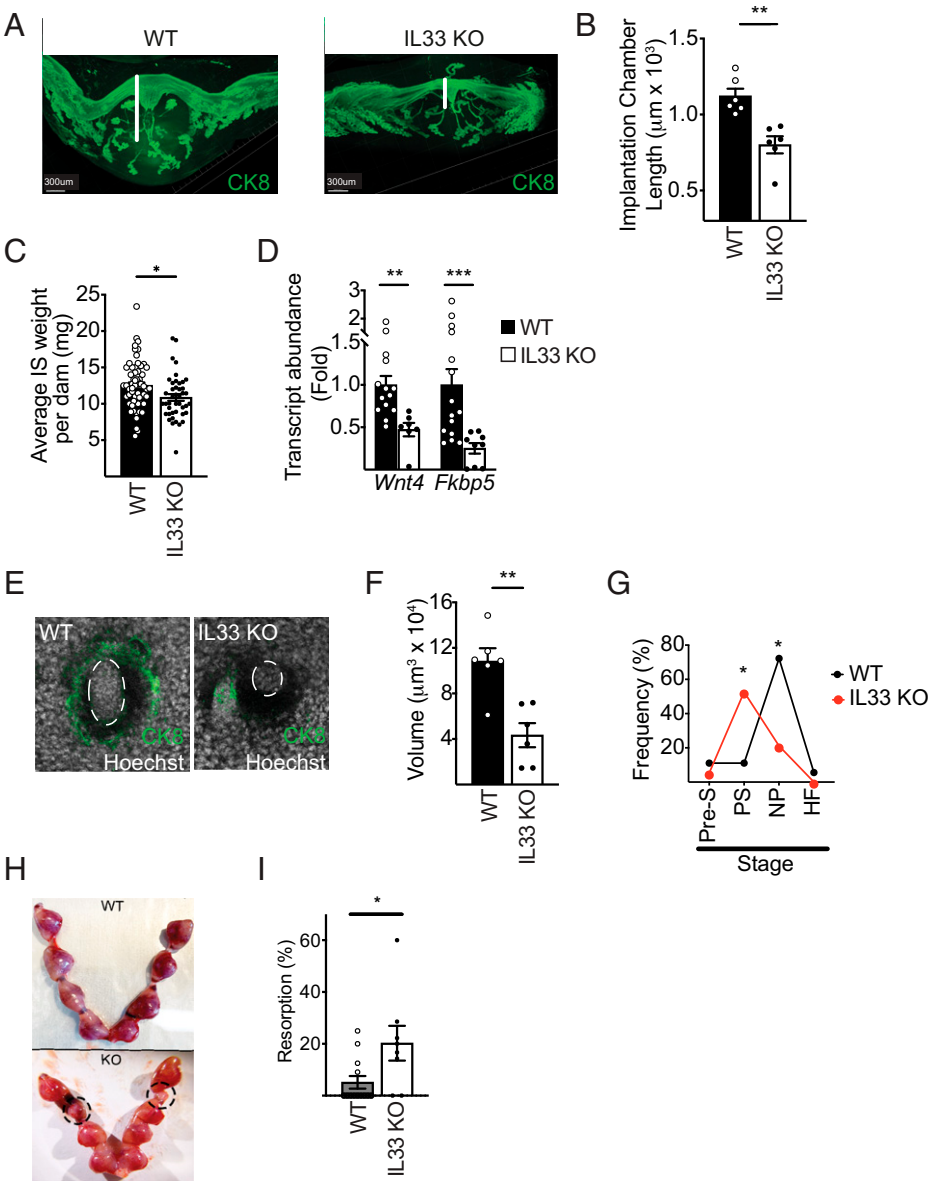

Fig. 2. Maternal IL-33 deficiency impairs implantation chamber formation, decidualization, and embryonic development in early pregnancy. (*A*) Reconstructed image of an implantation chamber from WT and IL-33 KO dams at E5.5 by confocal microscopy. Cytokeratin 8 (CK8, green) staining shows uterine epithelium. White lines indicate implantation chamber length. (*B*) Implantation chamber length in WT and IL-33 KO dams (n = 6 per group) at E5.5 by confocal microscopy as in *A*. (*C*) Average IS weight per dam from WT (n = 62) and IL-33 KO (n = 43) dams at E7.5. (*D*) Normalized *Wnt4* and *Fkbp5* transcript abundance in decidua from WT and IL-33 KO dams at E7.5 by qRT-PCR. Data points show two or three individual ISs from WT (n = 6) and IL-33 KO (n = 3) dams. (*E*) Reconstructed images of an embryo (white circles) within the implantation chamber from WT and IL-33 KO dams at E5.5 by confocal microscopy. Cytokeratin 8 (green) shows uterine epithelium encircling the chamber. Hoechst (white) shows nuclei. (*F*) Embryo volume in WT and IL-33 KO dams (n = 6 dams per group) at E5.5, measured by confocal microscopy after 3D reconstruction as in *A*. (*G*) Frequency of embryos at prestreak (Pre-S), primitive streak (PS), neural plate (NP), and headfold (HF) stages in WT (n = 18) and IL-33 KO (n = 19) dams at E7.5. (*H*) Images of uteri from WT and IL-33 KO dams at E12.5 showing resorptions in black circles. (*I*) Frequency of resorptions in WT (n = 13) and IL-33 KO (n = 8) dams at E12.5, identified as in *H*. Significance was determined by unpaired two-tailed Student's t test (*B*, *C*, and *F*), unpaired two-tailed Mann–Whitney U test (*D*), or Fisher's exact test (*G* and *I*) (*P < 0.05, **P < 0.01, ***P < 0.001). Data are displayed as mean ± SEM.

responses, such as natural killer (NK) cells and CD8$^+$ T cells, in certain tissues and immunological settings (19). To better understand how IL-33 regulates immune responses at the maternal–fetal interface during pregnancy, we first sought to define the uterine immune cell subsets that express ST2 at E7.5, a time point associated with significant, multifactorial defects in uterine tissue and vessel remodeling in IL-33 KO dams. As an unbiased approach to identify immune cells that express *Il1rl1* (encoding ST2), we performed scRNA-seq on CD45$^+$ immune cells sort-purified from the myometrium and decidua of WT dams at E7.5. The overall frequency of *Il1rl1*-expressing immune cells was relatively low in both tissues (Fig. 5 *A* and *D*), consistent with findings in other tissues. To better ascertain the identity of these subsets, *Il1rl1*-expressing cells were bioinformatically selected and reclustered (Fig. 5 *A* and *D*), revealing four distinct clusters of *Il1rl1*$^+$ cells in the myometrium (Fig. 5*B*) and three clusters in the decidua (Fig. 5*E*).

Among the four clusters in the myometrium, cells in cluster 1 exhibited higher expression of genes associated with a cDC2 identity, including major histocompatibility complex class II–related genes, *Itgax*, *Sirpa*, *Siglecg*, *Cd209a*, and *Clec10a* (Fig. 5*C*). Cluster 2 was enriched for genes associated with an ILC2 and/or T cell identity, for example, *Cd3g*, *Gata3*, *Bcl11b*, *Il7r*, *Thy1*, *Il2ra*, *Il5*, and *Rora* (Fig. 5*C*). Cluster 3 exhibited

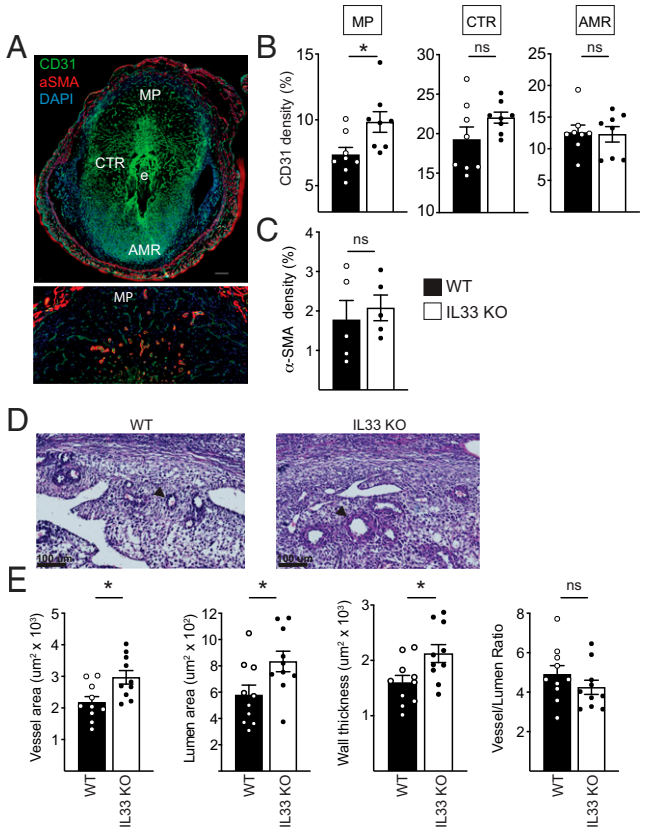

Fig. 3. IL-33 KO dams exhibit abnormal uterine vasculature and impaired SpA remodeling in early pregnancy. (*A*) Representative 20× image (*Top*) of CD31, αSMA, and DAPI in an IS from a WT dam at E7.5 (representative of $n = 8$ dams). (Scale bar, 200 μm.) MP, mesometrial pole; CTR, central region; e, embryo; AMR, anti-mesometrial region. Image (40×) (*Bottom*) of CD31, αSMA, and DAPI in MP of decidua from a WT dam at E7.5 (representative of $n = 5$ dams). (*B*) Signal density of $CD31^+$ vessels in the MP, CTR, and AMR of the decidua from WT ($n = 8$) and IL-33 KO ($n = 8$) dams at E7.5. Data points reflect individual dams. (*C*) Signal density of αSMA^+ vessels in the MP of the decidua from WT and IL-33 KO dams ($n = 5$ dams per group) at E7.5, identified as in *A*, *Bottom*. (*D*) Images (40×) of H&E staining of SpAs (black arrowheads) from WT and IL-33 KO dams at E9.5. (Scale bars, 100 μm.) (*E*) SpAs in ISs from WT ($n = 5$, 2 ISs per dam) and IL-33 KO ($n = 5$, 2 ISs per dam) dams at E9.5 were assessed for vessel and lumen area, wall thickness, and vessel-to-lumen ratio. Significance was determined by unpaired two-tailed Student's *t* test (*$P < 0.05$; ns, not significant). Data are displayed as mean ± SEM.

increased expression of genes associated with an M2 macrophage identity, including *Adgre1*, *Itgam*, *Lyz2*, *Sirpa*, *Egr2*, and *Mrc1* (Fig. 5*C*). And finally, cluster 4 had high expression of genes associated with mast cells, including *Il4*, *Cpa3*, *Gata2*, *Cma1*, *Mcpt4*, and *Fcer1a* (Fig. 5*C*).

Similar populations of $Il1rl1^+$ cells were identified in the decidua, with a few minor differences. Cells in cluster 1 expressed genes associated with both cDC2s and/or M2 macrophages (e.g., *Mgl2*, *Cd14*, *Cd68*, *Lyz2*, *Itgax*, and *Cd209a*), suggesting both cell subsets may be present in the cluster (Fig. 5*F*). Cluster 2 contained cells that expressed genes associated with a Treg and/or $CD4^+$ T cell identity (*Cd4*, *Cd3e*, *Cd3d*, *Cd3g*, *Ctla4*, *Il2ra*, and *Foxp3*), although a clear ILC2 signature was not apparent (Fig. 5*F*). And finally, cells in cluster 3 were enriched for mast cell genes (Fig. 5*F*). Of note, none of the clusters in the myometrium or decidua exhibited an NK cell or $CD8^+$ T cell gene signature, suggesting that IL-33 signaling may not directly regulate immune cells associated with type 1 immune responses at E7.5.

In summary, our data indicate that myeloid and lymphocyte populations associated with type 2 inflammation and/or tissue-remodeling responses (i.e., cDC2s, M2 macrophages, mast cells, Treg and non-Treg $CD4^+$ T cells, and ILC2s) are the principal IL-33–responsive immune cell subsets present in the decidualized uterus during early pregnancy.

Maternal IL-33 Deficiency Impairs Type 2 Responses by ILC2s, $CD4^+$ T Cells, and Macrophages in the Uterus during Early Pregnancy. IL-33 is a potent inducer of type 2 and tissue remodeling–associated immune responses by ILC2s and $CD4^+$ T cells in other tissues, including the lung, skin, adipose, and muscle (19, 20). We therefore hypothesized that IL-33 may similarly impact uterine ILC2 and $CD4^+$ T cell responses during early pregnancy. Consistent with our scRNA-seq data, flow cytometry studies revealed that the majority (~80 to 95%) of $ST2^+$ lymphocytes ($ST2^+FSC^{low}SSC^{low}CD90.2^+$ cells) in the myometrium at E7.5 (Fig. 6*A*) and E9.5 (*SI Appendix*, Fig. S6*A*) were ILC2s, although small populations of ST2-expressing $Foxp3^-CD4^+$ T cells and $Foxp3^+CD4^+$ Tregs were also detected. In the decidua, most $ST2^+$ lymphocytes were $Foxp3^+CD4^+$ Tregs or $Foxp3^-CD4^+$ T cells at E7.5, and few were ILC2s (~10%) (Fig. 6*A*). However, by E9.5, ILC2s were more frequent than CD4 T cells within the overall $ST2^+$ lymphocyte compartment (*SI Appendix*, Fig. S6*A*). Thus, ILC2s and $CD4^+$ T cells at the maternal–fetal interface express ST2 and are receptive to IL-33–mediated activation signals.

To assess IL-33–mediated regulation of uterine ILC2 and $CD4^+$ T cell responses during early pregnancy, we first quantified uterine ILC2s, $CD4^+$ Tregs, and non-Treg $CD4^+$ T cells in IL-33 KO and WT dams, but did not detect any significant differences at E7.5 (*SI Appendix*, Fig. S6*B*) or E9.5 (*SI Appendix*, Fig. S6*C*). These findings suggest that IL-33 may be dispensable for type 2 lymphocyte expansion and/or recruitment into the uterus, at least at this stage of pregnancy. We next assessed the impact of maternal IL-33 deficiency on uterine ILC2 and $CD4^+$ T cell production of cytokines associated with type 2 inflammatory and/or tissue-remodeling responses, including IL-5, IL-13, and AREG. These studies revealed that IL-5 and IL-13 production by ILC2s in the myometrium was reduced in IL-33 KO dams compared with WT dams at E7.5 and/or E9.5 (Fig. 6 *B* and *C* and *SI Appendix*, Fig. S7*A*). Similarly, IL-13 production by $Foxp3^-CD4^+$ T cells (Fig. 6*D* and *SI Appendix*, Fig. S7*B*) in the myometrium, and AREG production by $Foxp3^-CD4^+$ T cells in the decidua (*SI Appendix*, Fig. S7*C*), were also reduced in IL-33 KO dams compared with WT dams. Consistent with impaired local production of type 2 cytokines, decidual eosinophils were less abundant in IL-33 KO dams, as compared with WT dams, at E7.5 and E9.5 (Fig. 6*E*). Taken together, our data suggest that maternal IL-33 supports type 2 cytokine production by innate and adaptive lymphocytes in the uterus during the post-implantation phase of early pregnancy, prior to formation of the definitive placenta.

We next assessed responses by uterine Tregs at E7.5 and E9.5. AREG production by uterine Tregs from IL-33 KO and WT dams was similar, and we were unable to detect production of IL-10, IL-5, IL-13, or interferon γ by Tregs by intracellular cytokine staining (*SI Appendix*, Fig. S8). Moreover, although Tregs are critical for maintaining fetal tolerance in allogeneic pregnancies in mice (41–43), we find that defects in pregnancy progression are not exacerbated in IL-33 KO dams during allogeneic pregnancies, at least at E12.5 (*SI Appendix*, Fig. S9). Thus, our studies suggest that IL-33 may be dispensable for regulating the Treg functions that support fetal tolerance in allogeneic pregnancies.

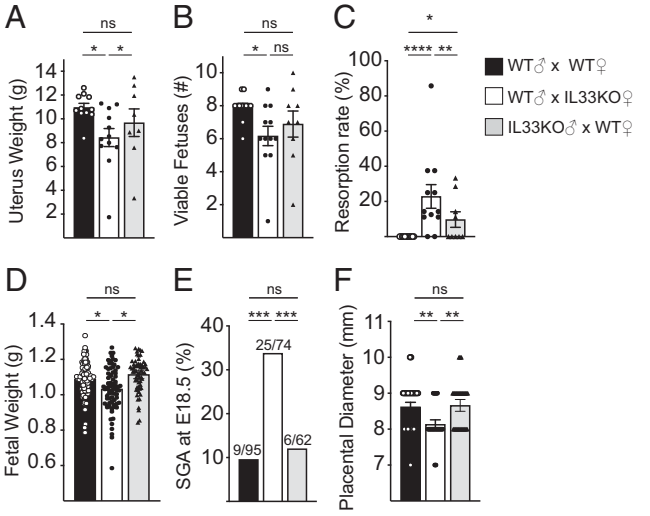

Fig. 4. Maternal IL-33 deficiency results in poor pregnancy outcome parameters in late pregnancy. Pregnancy outcome parameters were measured at E18.5 from WT (n = 12) and IL-33 KO dams (n = 12) mated with WT sires or from WT dams (n = 9) mated with IL-33 KO sires. Bar graphs show summary data as follows. (*A*) Uterus weight. (*B*) Number of viable fetuses. (*C*) Frequency of resorptions. (*D*) Fetal weight. (*E*) Frequency of SGA fetuses, defined as weighing less than 10th percentile of fetuses from WT × WT pregnancies. (*F*) Placental diameter. Significance was determined by one-way ANOVA (*A*), Kruskal–Wallis test with post hoc t tests (*B*), Fisher's exact test (*C* and *E*), or mixed-effects model analysis of repeated measures, with dam as subject (*D* and *F*) (*P < 0.05, **P < 0.01, ***P < 0.001, ****P < 0.0001; ns, not significant). Data are displayed as mean ± SEM.

Prior studies have implicated M2-like macrophages in uterine tissue remodeling during pregnancy (44–46). IL-33 is known to promote M2 polarization in many tissues, both directly via engagement of ST2 on specific macrophage subsets and indirectly by inducing production of type 2 cytokines such as IL-13 by ST2$^+$ lymphocytes (47, 48). Given our findings that some uterine macrophages express *Il1rl1* transcripts (Fig. 5 *C* and *F*) and that IL-33 regulates type 2 cytokine production by uterine lymphocytes (Fig. 6 *B*–*D* and *SI Appendix*, Fig. S7), we hypothesized that IL-33 signaling may directly or indirectly promote M2 macrophage function during early pregnancy. Consistent with this hypothesis, the number of decidual and myometrial macrophages expressing Arginase-1 (Arg-1), an enzyme associated with type 2–associated immune responses by M2 macrophages (49), was significantly reduced in IL-33 KO dams compared with WT dams at E7.5 (Fig. 6*F*). Thus, our data suggest that maternal IL-33 signaling regulates M2 macrophage function during early pregnancy in mice, coincident with IL-33–dependent remodeling of the uterine tissue and vasculature.

Discussion

Our studies demonstrate that IL-33 critically regulates diverse aspects of pregnancy progression in mice. We find that maternal IL-33 deficiency impairs implantation chamber development and uterine decidualization, and perturbs vascularization and vascular remodeling, in the post-implantation period of early pregnancy. These defects coincide with delayed embryo development at E5.5 and E7.5, increased resorption rates, and impairments in fetal and placental growth by late pregnancy. At a cellular level, our data suggest that crosstalk between IL-33–producing nonimmune cells and ST2$^+$ immune cells at the maternal–fetal interface is associated with optimal pregnancy progression. Specifically, we find that myometrial fibroblasts and myofibroblasts, and decidual endothelial and stromal cells, are the main cellular sources of IL-33 in the decidualized uterus. Conversely, ST2 is expressed by uterine immune cell populations associated with type 2 immune responses, including ILC2s, some Tregs and conventional CD4$^+$ T cells, cDC2s, M2-polarized macrophages, and mast cells. Critically, the early defects in uterine tissue remodeling and embryo development in pregnant IL-33 KO dams were associated with broadly impaired type 2 immune responses, including diminished type 2 cytokine production by uterine lymphocytes and reduced numbers of uterine eosinophils and Arginase-1$^+$ macrophages at E7.5. Taken together, our studies highlight previously unappreciated roles for IL-33 in orchestrating key tissue remodeling and immunological processes at the maternal–fetal interface that collectively support early pregnancy progression and optimal pregnancy outcomes in mice.

Our data demonstrate that maternal IL-33 deficiency has pleiotropic effects on early pregnancy progression, resulting in diverse defects in the post-implantation, pre-placentation phase of early pregnancy. However, whether and how IL-33 supports events that precede implantation are less clear. While we find that total implantation site numbers at E7.5 are reduced in IL-33 KO dams, the modest nature of this reduction suggests that IL-33 may play relatively minor roles in the reproductive processes that are required to initiate implantation in mice—such as oogenesis and oocyte release during estrus, oocyte fertilization, and blastocyst attachment—notwithstanding our prior finding that IL-33 is expressed in the ovaries and uteri of virgin mice and through E2.5 in pregnancy (50).

The relative, stage-specific requirements for IL-33 in early pregnancy progression may reflect differences in the uterine cell types that express IL-33 in the pre- versus post-implantation stages of early pregnancy. For example, we have previously shown that glandular and luminal epithelial cells are the main IL-33$^+$ cells in the endometrium at E2.5 (50), whereas we now show that stromal cells and endothelial cells are the main IL-33$^+$ cell types in the decidua during the post-implantation stage of early pregnancy, although IL-33 expression by decidual endothelial cells during this time frame is transient and peaks at E7.5. Our findings are consistent with a recent scRNA-seq study on mouse implantation sites at E5.5, which identified *Il33* transcripts in *Hoxa11*-positive decidual stromal cells arising during the "second wave" of decidualization that follows blastocyst implantation (51). Although future studies involving cell-specific and temporal disruption of IL-33 are necessary to define the relative and sequential contributions of epithelial-, endothelial-, and stromal cell–derived IL-33 to early pregnancy progression, one possibility is that IL-33 produced by decidualizing stromal cells may amplify uterine decidualization and other decidual processes following blastocyst implantation, possibly after processing into its highly bioactive, mature ∼20-kDa form. This idea is supported by prior literature showing that IL-33 can regulate expression of genes associated with differentiation, proliferation, and function in human decidual cells and trophoblasts in vitro (52, 53), and our current finding that maternal loss of IL-33 signaling significantly impairs decidual expression of *Wnt4* and *Fkbp5*. Notably, both genes are known mediators of BMP2 signaling, which critically supports early pregnancy in mice and humans by promoting uterine stromal cell decidualization and proliferation (54, 55).

We find that IL-33–dependent type 2 immune responses in the uterus are closely associated with proper tissue remodeling during early pregnancy. Moreover, our data are consistent with the emerging paradigm that crosstalk between IL-33$^+$ non-immune and ST2$^+$ immune cells instructs tissue remodeling and repair processes in diverse physiological and pathological settings. For

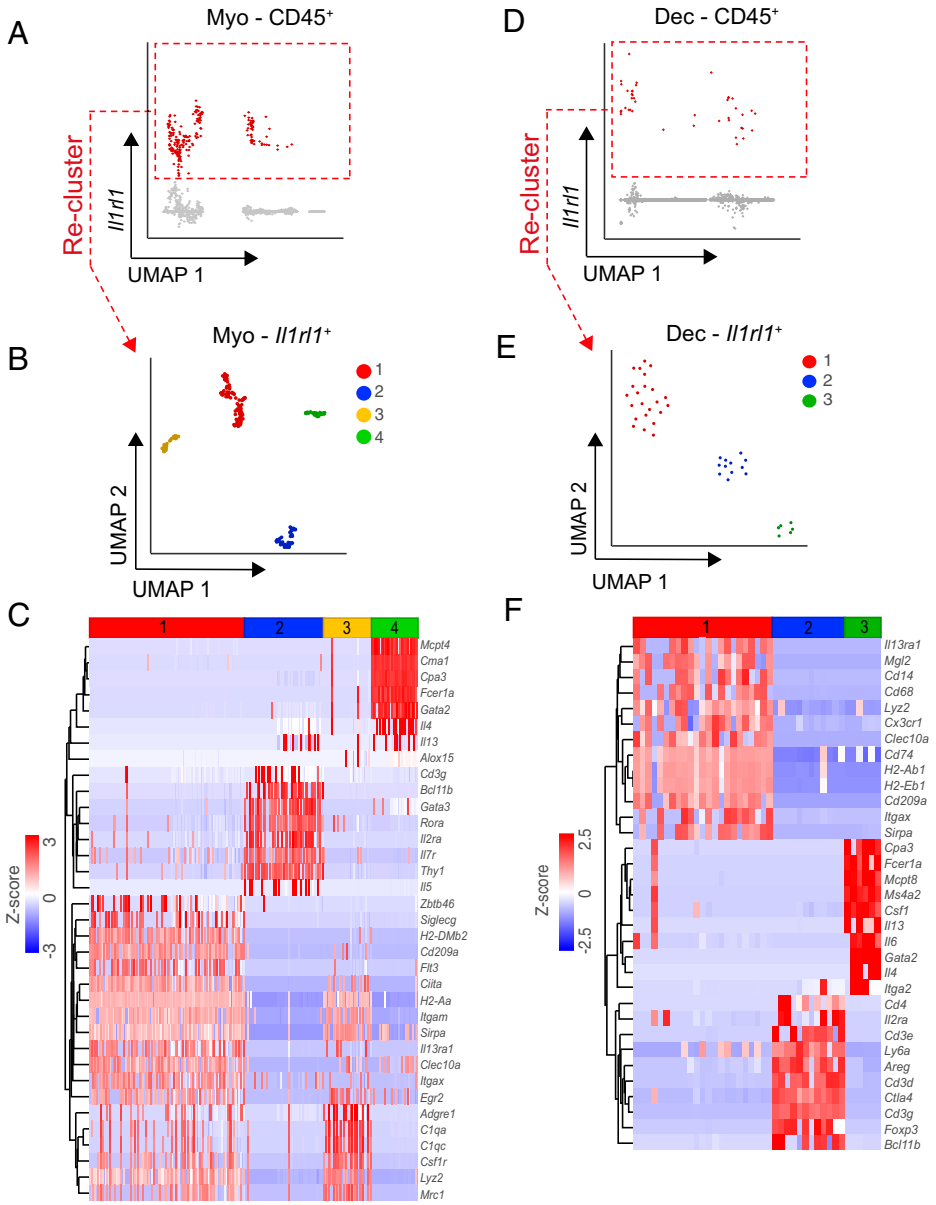

Fig. 5. *Il1rl1* is expressed by type 2 immune cells in the uterus at E7.5. (*A* and *D*) UMAP of scRNA-seq data showing normalized *Il1rl1* expression in individual live CD45$^+$ cells purified from the myometrium (*A*) or decidua (*D*) of implantation sites from WT dams at E7.5 (n = 2 dams, 8 pooled ISs per dam). (*B* and *E*) *Il1rl1*$^+$ cells in Myo (*B*) and Dec (*E*) were reclustered by *K*-means clustering and visualized by UMAP. (*C* and *F*) Heatmaps showing select differentially expressed genes (false discovery rate <0.5, fold >2 or <−2) among the distinct clusters of *Il1rl1*$^+$ cells in the Myo (*C*) and Dec (*F*).

example, epithelial cell–derived IL-33 has been shown to drive tissue-reparative type 2 immune responses by ILC2s, T cells, and myeloid cells in the infected lung, inflamed gut, and injured skin (19, 20). Similarly, fibroblast-derived IL-33 activates ST2$^+$ skeletal muscle Tregs to elicit production of cytokines, including AREG, which promote muscle satellite cell proliferation and differentiation to repair injured muscle tissue (56, 57), a function that may have relevance to our finding that IL-33$^+$ myofibroblasts and ST2$^+$ immune cells are highly enriched in the myometrium. IL-33–dependent type 2 immune responses also support tissue homeostasis under physiologic conditions, as demonstrated by the finding that astrocyte-derived IL-33 in the central nervous system instructs synapse engulfment by ST2$^+$ microglia to remodel neural networks during postnatal development (58). Our data do not exclude the possibility that IL-33 may impact pregnancy outcomes by exerting effects on organs and systems other than the uterus, which are nonetheless critical for a successful pregnancy (e.g., the cardiovascular system or kidneys). Nevertheless, given the broader role of type 2 immune responses in tissue remodeling in many other organs, our data suggest that local IL-33–induced type 2 immune responses in the uterus may similarly contribute to uterine remodeling during early pregnancy.

In addition to decidual stromal cells, we find that blood vessels in the mesometrial pole express IL-33 at E7.5. This finding mirrors prior reports of IL-33 expression by endothelial cells in many other tissues (59–61), including in the human placenta at midgestation (62). Our data suggest that IL-33 may play dual roles in regulating vascular remodeling in the uterus during early pregnancy, acting to limit the density of vessels in the mesometrial pole at E7.5 and to restrict the wall thickness and gauge of SpAs at E9.5. The cellular mechanisms underlying this negative regulatory function remain unclear. IL-33–mediated crosstalk between non-immune and immune cells in "adventitial cuffs" surrounding large blood vessels can promote type 2 inflammatory responses in other tissues (63). In the uterus, decidual NK cells, Tregs, and mast cells have all been

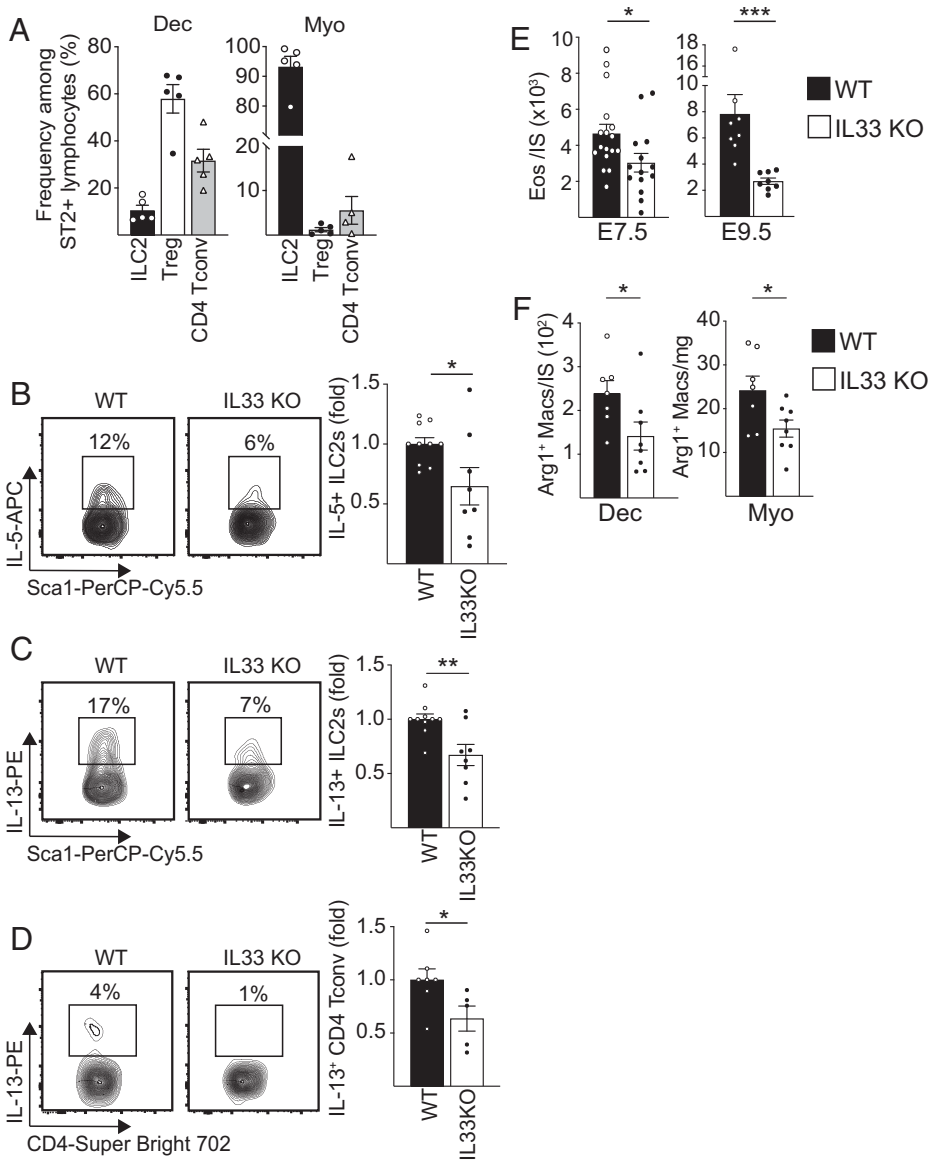

Fig. 6. Maternal IL-33 promotes type 2 immune responses by uterine immune cells during early pregnancy. (*A*) Percentage of ILC2s, $CD4^+Foxp3^+$ T cells (Tregs), and $CD4^+Foxp3^-$ (Tconv) in the Dec and Myo among $ST2^+$ lymphocytes from WT dams at E7.5 by flow cytometry (n = 5 dams, 6 to 9 pooled ISs per dam). (*B*) Representative flow plot (*Left*) showing the percentage of $IL\text{-}5^+$ ILC2s from the myometrium of WT and IL-33 KO dams at E7.5 by flow cytometry. Summary data (*Right*) for WT (n = 10 dams, 7 to 11 pooled ISs per dam) and IL-33 KO (n = 8 dams, 7 to 12 pooled ISs per dam) from seven independent experiments, shown as fold change relative to average for the WT group in each experiment. (*C*) As in *B*, except showing IL-13. (*D*) As in *C*, except showing $IL\text{-}13^+CD4^+$ T cells from WT (n = 7 dams, 7 to 11 pooled ISs per dam) and IL-33 KO dams (n = 5, 7 to 12 pooled ISs per dam) at E7.5. Significance was determined by two-tailed Student's t test. (*E*) Number of eosinophils in the decidua at E7.5 (*Left*) and E9.5 (*Right*) from WT dams (n = 8 to 17, 5 to 11 pooled ISs per dam) and IL-33 KO dams (n = 8 to 14, 6 to 10 pooled ISs per dam), shown as the number per IS. Significance was determined by unpaired two-tailed Mann–Whitney U test. (*F*) Number of Arginase-1^+ macrophages in the decidua (*Left*) and myometrium (*Right*) from WT (n = 7 dams, 6 to 11 pooled ISs per dam) and IL-33 KO dams (n = 8 dams, 7 to 9 pooled ISs per dam) at E7.5. Shown as the number per IS or number per milligram of tissue. Significance was determined by unpaired two-tailed Student's t test (*P < 0.05, **P < 0.01, ***P < 0.001). Data are displayed as mean ± SEM.

implicated in remodeling of the uterine vasculature during pregnancy (64–66). For example, decidual NK cells are known to localize near blood vessels in the mesometrial pole and secrete factors that support SpA remodeling and angiogenesis (67). It will be important to determine whether IL-33 limits decidual angiogenesis or SpA remodeling by modulating the pro-vasculature functions of decidual NK cells, Tregs, and/or mast cells, possibly through induction of type 2 cytokines and inflammatory mediators. Our data raise the intriguing possibility that IL-33–producing endothelial cells in the mesometrial pole engage in crosstalk with vessel-adjacent $ST2^+$ immune cells—for example, T cells, mast cells, or even ILC2s—to directly or indirectly regulate secretion of factors that alter vessel growth and architecture.

Although this study is focused on how IL-33 signaling contributes to pregnancy in mice, our findings may shed light on why abnormalities in IL-33 signaling are associated with a broad spectrum of pregnancy disorders and poor pregnancy outcomes in humans (4, 5, 7–17, 68, 69). Indeed, several key findings from our work parallel observations from studies on women with pregnancy disorders. For example, our data demonstrate that IL-33 KO dams exhibit increased resorptions at mid- and late gestation, similar to reports of abnormal IL-33 signaling in women with recurrent or pending miscarriage (4, 5, 15, 16). Additionally, we find that IL-33 is predominantly expressed by uterine fibroblasts/myofibroblasts and decidual stromal and endothelial cells in the post-implantation phase of early pregnancy in mice. Similar cell types have been

reported to express IL-33 in women, including during pregnancy (8, 14, 52, 62, 70). And finally, dysregulated IL-33 signaling in patients with recurrent pregnancy loss is associated with reduced expression of M2 markers by human decidual macrophages (68), mirroring our own findings of impaired M2 macrophage responses in IL-33 KO dams. Taken together, these findings suggest that IL-33 may support pregnancy progression in both humans and mice via conserved cellular communication networks and functions.

Finally, although prior work had shown that IL-33 contributes to protection against LPS-induced complications and preterm labor at late gestation in mice and rats (17, 18), we now demonstrate that IL-33 acts very early in pregnancy to critically regulate the tissue and vascular remodeling processes that establish the foundation for proper development and function of the placenta. This early role for IL-33 could impact, and possibly explain, some of the complications that arise at later stages of pregnancy in LPS-challenged rodents and in women with diverse pregnancy disorders.

In summary, our study demonstrates that IL-33 signaling has pleiotropic effects on diverse physiological, cellular, and immunological processes in the pregnant uterus that are important for optimal pregnancy progression and outcomes in mice. Future studies are needed to determine whether uterine $ST2^+$ immune cells directly participate in IL-33–mediated responses promoting decidualization and vascularization in early pregnancy. Finally, our work also provides insights into the cellular and molecular mechanisms that could be involved in dysregulated IL-33 signaling and poor pregnancy outcomes in women.

Methods

Animals and Breeding. C57BL/6 WT mice (Jackson) and IL-33 Citrine fluorescent reporter ($Il33^{cit/wt}$) or KO ($Il33^{cit/cit}$) mice on a C57BL/6 background (26) were used for all experiments, except that BALB/c WT males (Jackson) were used as studs for the allogeneic mating studies. All mice were used in accordance with the Rutgers Institutional Animal Care and Use Committee. To initiate pregnancies, 8- to 12-wk-old females in estrus were paired with male C57BL/6 studs (or with BALB/c studs for allogeneic pregnancy studies) in the late afternoon. The presence of a vaginal plug the next morning marked E0.5 of pregnancy. Dams were euthanized by CO_2 asphyxiation unless otherwise noted.

Histology and Immunofluorescence with Two-Dimensional Imaging. For histology, E7.5 implantation sites (ISs) with myometrium attached were fixed in Bouin's solution (Sigma), paraffin-embedded, sectioned at 7 μm, and stained with hematoxylin and eosin (H&E). Embryos in one to three ISs per dam were assessed to identify morphologic landmarks of prestreak, primitive streak, neural plate, and headfold stages of embryonic development, as in ref. 36. All sections having an implantation chamber were scored by three observers for the number of cavities within the embryo and the presence or absence of traits, including primitive streak, allantois, cranial neural folds, and somites. Embryonic stage was based on the composite of these traits.

For placental morphology analysis at E18.5, placentas were hemisected and fixed in Bouin's solution (Sigma), paraffin-embedded, sectioned at 7 μm, and stained with H&E. The total areas of labyrinth and junctional zone were measured at 20× with ImageJ v1.52 (NIH).

For 2D immunofluorescence, ISs with myometrium attached were fixed in 4% paraformaldehyde (PFA) (Sigma) at 4 °C, infiltrated with 30% sucrose (Sigma) in phosphate-buffered saline, embedded in Tissue-Tek O.C.T. compound (Sakura), and cryosectioned at 7 μm. Immunostaining was performed, as described (50), using antibodies listed in *SI Appendix*, Table S1. Two or three ISs per dam were analyzed, using at least three sections per IS. Purified goat or rabbit immunoglobulin G was used as isotype-specific negative controls and primary antibodies were omitted to detect nonspecific binding of secondary antibodies. Vectashield with DAPI (Vector) was used for nuclear visualization and mounting. CD31 and αSMA signal density in the decidua were calculated using ImageJ v1.52 (NIH), as described (39). Briefly, individual images were corrected by subtracting the background intensity using the autothreshold function. For four (mesometrial pole and central region at 20×) or eight (antimesometrial region at 40×) nonoverlapping 300 × 300 pixel regions, signal density was calculated as the percentage of signal-positive area [e.g., (αSMA^+ pixels/total pixels in region) × 100% = percent αSMA signal density]. One IS per dam was analyzed; all measurements from three separate sections per IS were averaged.

Imaging was performed on a BZ-X710 All-in-One fluorescence microscope (Keyence) using Keyence BZ-X Viewer v01.03 software.

Spiral Artery Remodeling. SpA remodeling was assessed at E9.5 as described (71). Briefly, dams were euthanized by cervical dislocation and uterine arteries were ligated at distal and proximal ends. The whole uterus was excised and fixed in 4% PFA for 5 h at room temperature. Isolated ISs were paraffin-embedded and sectioned at 7 μm. H&E staining on sections at 49-μm intervals was used to identify sections containing the chorioallantoic attachment of the fetus to the placenta, defining the midsagittal point of the feto–placental unit. Three sections, spaced 49 μm apart and close to the midsagittal point, were analyzed for each IS. Using NIS Elements software, total vessel and lumen area were determined by drawing around the outer wall and the inside of the vessel, respectively. Measurements were recorded from five of the largest and roundest vessels within the center 2/4 of the decidua of the feto–placental unit. The 15 measurements were averaged to yield the mean diameter of the largest vessels per IS. Wall thickness was calculated by subtracting lumen area from total vessel area. Vessel:lumen ratio and wall thickness reflect the remodeling status of the vessel. Two ISs per dam were analyzed.

Tissue Digestion. Single-cell suspensions were generated as previously described (39). Briefly, the myometrium and decidua from individual ISs were separated and minced with scissors, and then digested in RPMI-1640 (Gibco) containing 1 mg/mL collagenase A (Sigma-Aldrich) and 0.1 mg/mL DNase (Roche) with shaking at 250 rpm at 37 °C for 2 × 12 min (decidua) or 2 × 15 min (myometrium). Tissues were mechanically dissociated by passage through an 18- or 20-gauge needle after each shaking cycle. Cells were filtered through 100-μm mesh and washed once with cold RPMI with 3% fetal bovine serum (FBS) (Fisher Scientific). Red blood cells were lysed with RBC lysis buffer (Tonbo Biosciences).

Flow Cytometry and Cell Sorting. Flow cytometry was performed using antibodies listed in *SI Appendix*, Table S2. Cells were stained with Live/Dead Fixable Aqua viability dye (Invitrogen) for 30 min per the manufacturer's instructions prior to surface staining, or with DAPI after surface staining for cell sorting. Cells were treated with Fc Block (BD Biosciences) for 10 min, and then surface-stained with antibody mixture for 30 min at 4 °C. The Foxp3/Transcription Factor Staining Kit (eBioscience) was used for intracellular or intranuclear staining. Lineage mixture included anti-CD3, -CD19, -CD11b, -CD11c, -NK1.1, -CD8, –Ter-119, and -FcERI. ILC2s were identified as $CD45^+LIN^-CD90.2^+Sca1^+CD25^+ST2^+$ cells, eosinophils as $CD45^+SiglecF^+F4/80^{lo}SSC^{hi}$ cells, and macrophages as $CD45^+CD11b^{hi}F4/80^{hi}CD64^{hi}$ cells. An Attune NxT acoustic focusing cytometer (Thermo Fisher) and a FACSAria II sorter (BD Biosciences) were used for flow cytometry and cell sorting, respectively. Data were analyzed using FlowJo v10 software (BD Biosciences).

In Vitro Stimulation. Single-cell suspensions were incubated at 37 °C for 5 h with Cell Activation Cocktail with brefeldin A (BioLegend) or GolgiPlug (BD Biosciences), per the manufacturer's instructions, in RPMI-1640 medium (Gibco) containing 1% Hepes (Corning), 1% penicillin-streptomycin (Corning), and 10% FBS (Fisher Scientific).

Statistical Analyses. Statistical analyses were performed with Prism v9 (GraphPad Software). Outliers were identified and removed. Normality was determined using the Shapiro–Wilk test. Significant differences were determined using unpaired two-tailed Student's *t* test for normally distributed data, Mann–Whitney *U* test for nonparametric data, or Fisher's exact test for binary data. When comparing more than two groups, one-way ANOVA or Kruskal–Wallis test with post hoc *t* test was used. Fetal and placental

weight, fetal:placental weight ratio, and placental diameter were analyzed by mixed-effects model analysis of repeated measures and post hoc *t* test, with dam as subject and viable fetuses as repeated measures. All bar graphs show mean ± SEM and significance is reported as $*P < 0.05$, $**P < 0.01$, $***P < 0.001$, unless otherwise stated in the legends.

Additional Methods. Methods for scRNA-seq processing and data analyses, qRT-PCR, whole-mount immunofluorescence with 3D reconstruction studies, and Western blots are available in *SI Appendix*.

Data, Materials, and Software Availability. scRNA-seq data reported in this article have been deposited in the Gene Expression Omnibus [accession nos. GSE209795 (72) and GSE209796 (73)].

All other data are included in the manuscript and/or *SI Appendix*.

ACKNOWLEDGMENTS. We thank Mark Siracusa and Joseph Sun for helpful discussions and feedback. We thank the Rutgers Flow Cytometry Core for instrumentation use, the Rutgers Genomics Core for generating raw scRNA-seq data, and Alexander Lemenze for generating processed scRNA-seq data in Cell Ranger. This research was supported by National Institute of Allergy and Infectious Diseases–NIH Grant R01AI148695 (to A.M.B. and N.C.D.) and March of Dimes Grant 5-FY20-209 (to R.A.). The content is solely the responsibility of the authors and does not necessarily represent the official views of the NIH.

Author affiliations: [a]Center for Immunity and Inflammation, New Jersey Medical School, Rutgers Biomedical and Health Sciences, Rutgers - The State University of New Jersey, Newark, NJ 07103; [b]Department of Microbiology, Biochemistry, and Molecular Genetics, New Jersey Medical School, Rutgers Biomedical and Health Sciences, Rutgers - The State University of New Jersey, Newark, NJ 07103; [c]Institute for Quantitative Health Science and Engineering, Michigan State University, East Lansing, MI 48824; [d]Department of Obstetrics, Gynecology and Reproductive Biology, Michigan State University, East Lansing, MI 48824; [e]Cell and Molecular Biology Program, Michigan State University, East Lansing, MI 48824; [f]Rutgers School of Graduate Studies, Rutgers - The State University of New Jersey, Newark, NJ 07103; [g]Department of Obstetrics, Gynecology and Reproductive Health, New Jersey Medical School, Rutgers Biomedical and Health Sciences, Rutgers - The State University of New Jersey, Newark, NJ 07103; and [h]Department of Medicine, New Jersey Medical School, Rutgers Biomedical and Health Sciences, Rutgers - The State University of New Jersey, Newark, NJ 07103

1. F. Colucci, The immunological code of pregnancy. *Science* **365**, 862–863 (2019).
2. G. Mor, P. Aldo, A. B. Alvero, The unique immunological and microbial aspects of pregnancy. *Nat. Rev. Immunol.* **17**, 469–482 (2017).
3. M. PrabhuDas *et al.*, Immune mechanisms at the maternal-fetal interface: Perspectives and challenges. *Nat. Immunol.* **16**, 328–334 (2015).
4. H. E. Zidan, R. S. Abdul-Maksoud, H. E. Mowafy, W. S. H. Elsayed, The association of IL-33 and Foxp3 gene polymorphisms with recurrent pregnancy loss in Egyptian women. *Cytokine* **108**, 115–119 (2018).
5. J. Yue, Y. Tong, L. Xie, T. Ma, J. Yang, Genetic variant in IL-33 is associated with idiopathic recurrent miscarriage in Chinese Han population. *Sci. Rep.* **6**, 23806 (2016).
6. S. Soheilyfar *et al.*, Association of IL-10, IL-18, and IL-33 genetic polymorphisms with recurrent pregnancy loss risk in Iranian women. *Gynecol. Endocrinol.* **35**, 342–345 (2019).
7. H. Chen *et al.*, Decreased IL-33 production contributes to trophoblast cell dysfunction in pregnancies with preeclampsia. *Mediators Inflamm.* **2018**, 9787239 (2018).
8. I. Granne *et al.*, ST2 and IL-33 in pregnancy and pre-eclampsia. *PLoS One* **6**, e24463 (2011).
9. T. Stampalija *et al.*, Maternal plasma concentrations of sST2 and angiogenic/anti-angiogenic factors in preeclampsia. *J. Matern. Fetal Neonatal Med.* **26**, 1359–1370 (2013).
10. F. Beneventi *et al.*, Maternal and fetal leptin and interleukin 33 concentrations in pregnancy complicated by obesity and preeclampsia. *J. Matern. Fetal Neonatal Med.* **33**, 3942–3948 (2020).
11. İ. Eda Gökdemir *et al.*, Evaluation of ADAMTS12, ADAMTS16, ADAMTS18 and IL-33 serum levels in pre-eclampsia. *J. Matern. Fetal Neonatal Med.* **29**, 2451–2456 (2016).
12. S. Ozler, E. Oztas, B. G. Guler, A. T. Caglar, Increased levels of serum IL-33 is associated with adverse maternal outcomes in placenta previa accreta. *J. Matern. Fetal Neonatal Med.* **34**, 3192–3199 (2021).
13. W. Fan *et al.*, Interleukin-33 and its receptor soluble suppression of tumorigenicity 2 in the diagnosis of gestational diabetes mellitus. *Int. J. Clin. Pract.* **75**, e14944 (2021).
14. M. S. Salker *et al.*, Disordered IL-33/ST2 activation in decidualizing stromal cells prolongs uterine receptivity in women with recurrent pregnancy loss. *PLoS One* **7**, e52252 (2012).
15. T. J. Kaitu'u-Lino, L. Tuohey, S. Tong, Maternal serum interleukin-33 and soluble ST2 across early pregnancy, and their association with miscarriage. *J. Reprod. Immunol.* **95**, 46–49 (2012).
16. W.-T. Hu *et al.*, IL-33 enhances proliferation and invasiveness of decidual stromal cells by up-regulation of CCL2/CCR2 via NF-κB and ERK1/2 signaling. *MHR: Basic Sci. Reprod. Med.* **20**, 358–372 (2014).
17. B. Huang *et al.*, Interleukin-33-induced expression of PIBF1 by decidual B cells protects against preterm labor. *Nat. Med.* **23**, 128–135 (2017).
18. K. Kozai *et al.*, Protective role of IL33 signaling in negative pregnancy outcomes associated with lipopolysaccharide exposure. *FASEB J.* **35**, e21272 (2021).
19. F. Y. Liew, J. P. Girard, H. R. Turnquist, Interleukin-33 in health and disease. *Nat. Rev. Immunol.* **16**, 676–689 (2016).
20. A. B. Molofsky, A. K. Savage, R. M. Locksley, Interleukin-33 in tissue homeostasis, injury, and inflammation. *Immunity* **42**, 1005–1019 (2015).
21. C. Cayrol, J. P. Girard, Interleukin-33 (IL-33): A nuclear cytokine from the IL-1 family. *Immunol. Rev.* **281**, 154–168 (2018).
22. P. K. Mishra *et al.*, Sterile particle-induced inflammation is mediated by macrophages releasing IL-33 through a Bruton's tyrosine kinase-dependent pathway. *Nat. Mater.* **18**, 289–297 (2019).
23. C. Y. Ramathal, I. C. Bagchi, R. N. Taylor, M. K. Bagchi, Endometrial decidualization: Of mice and men. *Semin. Reprod. Med.* **28**, 17–26 (2010).
24. S.-P. Wu, O. M. Emery, F. J. DeMayo, Molecular studies on pregnancy with mouse models. *Curr. Opin. Physiol.* **13**, 123–127 (2020).
25. S.-W. Ng *et al.*, Endometrial decidualization: The primary driver of pregnancy health. *Int. J. Mol. Sci.* **21**, 4092 (2020).
26. C. S. Hardman, V. Panova, A. N. McKenzie, IL-33 citrine reporter mice reveal the temporal and spatial expression of IL-33 during allergic lung inflammation. *Eur. J. Immunol.* **43**, 488–498 (2013).
27. E. S. Cohen *et al.*, Oxidation of the alarmin IL-33 regulates ST2-dependent inflammation. *Nat. Commun.* **6**, 8327 (2015).
28. E. Lefrançais *et al.*, Central domain of IL-33 is cleaved by mast cell proteases for potent activation of group-2 innate lymphoid cells. *Proc. Natl. Acad. Sci. U.S.A.* **111**, 15502–15507 (2014).
29. I. G. Luzina *et al.*, Full-length IL-33 promotes inflammation but not Th2 response in vivo in an ST2-independent fashion. *J. Immunol.* **189**, 403–410 (2012).
30. M. B. Buechler *et al.*, Cross-tissue organization of the fibroblast lineage. *Nature* **593**, 575–579 (2021).
31. L. Muhl *et al.*, Single-cell analysis uncovers fibroblast heterogeneity and criteria for fibroblast and mural cell identification and discrimination. *Nat. Commun.* **11**, 3953 (2020).
32. P. Pakshir *et al.*, The myofibroblast at a glance. *J. Cell Sci.* **133**, jcs227900 (2020).
33. M. V. Plikus *et al.*, Fibroblasts: Origins, definitions, and functions in health and disease. *Cell* **184**, 3852–3872 (2021).
34. J.-P. He, Q. Tian, Q.-Y. Zhu, J.-L. Liu, Identification of intercellular crosstalk between decidual cells and niche cells in mice. *Int. J. Mol. Sci.* **22**, 7696 (2021).
35. R. Arora *et al.*, Insights from imaging the implanting embryo and the uterine environment in three dimensions. *Development* **143**, 4749–4754 (2016).
36. K. M. Downs, T. Davies, Staging of gastrulating mouse embryos by morphological landmarks in the dissecting microscope. *Development* **118**, 1255–1266 (1993).
37. C. Wang *et al.*, Expression of vascular endothelial growth factor by granulated metrial gland cells in pregnant murine uteri. *Cell Tissue Res.* **300**, 285–293 (2000).
38. M. Kim *et al.*, VEGF-A regulated by progesterone governs uterine angiogenesis and vascular remodelling during pregnancy. *EMBO Mol. Med.* **5**, 1415–1430 (2013).
39. N. M. Marchetto *et al.*, Endothelial Jagged1 antagonizes Dll4/Notch signaling in decidual angiogenesis during early mouse pregnancy. *Int. J. Mol. Sci.* **21**, 6477 (2020).
40. J. Zhang, Z. Chen, G. N. Smith, B. A. Croy, Natural killer cell-triggered vascular transformation: Maternal care before birth? *Cell. Mol. Immunol.* **8**, 1–11 (2011).
41. V. R. Aluvihare, M. Kallikourdis, A. G. Betz, Regulatory T cells mediate maternal tolerance to the fetus. *Nat. Immunol.* **5**, 266–271 (2004).
42. R. M. Samstein, S. Z. Josefowicz, A. Arvey, P. M. Treuting, A. Y. Rudensky, Extrathymic generation of regulatory T cells in placental mammals mitigates maternal-fetal conflict. *Cell* **150**, 29–38 (2012).
43. T. Shima *et al.*, Regulatory T cells are necessary for implantation and maintenance of early pregnancy but not late pregnancy in allogeneic mice. *J. Reprod. Immunol.* **85**, 121–129 (2010).
44. Y. Ono *et al.*, CD206$^+$ M2-like macrophages are essential for successful implantation. *Front. Immunol.* **11**, 557184 (2020).
45. V. Plaks *et al.*, Uterine DCs are crucial for decidua formation during embryo implantation in mice. *J. Clin. Invest.* **118**, 3954–3965 (2008).
46. E. Tagliani *et al.*, Coordinate regulation of tissue macrophage and dendritic cell population dynamics by CSF-1. *J. Exp. Med.* **208**, 1901–1916 (2011).
47. M. Kurowska-Stolarska *et al.*, IL-33 amplifies the polarization of alternatively activated macrophages that contribute to airway inflammation. *J. Immunol.* **183**, 6469–6477 (2009).
48. J. M. Lott, T. L. Sumpter, H. R. Turnquist, New dog and new tricks: Evolving roles for IL-33 in type 2 immunity. *J. Leukoc. Biol.* **97**, 1037–1048 (2015).
49. J. T. Pesce *et al.*, Arginase-1-expressing macrophages suppress Th2 cytokine-driven inflammation and fibrosis. *PLoS Pathog.* **5**, e1000371 (2009).
50. S. Begum *et al.*, Dynamic expression of interleukin-33 and ST2 in the mouse reproductive tract is influenced by superovulation. *J. Histochem. Cytochem.* **68**, 253–267 (2020).
51. Y. Yang, J.-P. He, J.-L. Liu, Cell-cell communication at the embryo implantation site of mouse uterus revealed by single-cell analysis. *Int. J. Mol. Sci.* **22**, 5177 (2021).
52. V. Fock *et al.*, Macrophage-derived IL-33 is a critical factor for placental growth. *J. Immunol.* **191**, 3734–3743 (2013).
53. X.-H. Wang *et al.*, IL-33 restricts invasion and adhesion of trophoblast cell line JEG3 by downregulation of integrin α4β1 and CD62L. *Mol. Med. Rep.* **16**, 3887–3893 (2017).
54. K. Y. Lee *et al.*, Bmp2 is critical for the murine uterine decidual response. *Mol. Cell. Biol.* **27**, 5468–5478 (2007).
55. H.-J. Zhao *et al.*, Bone morphogenetic protein 2 promotes human trophoblast cell invasion by inducing activin A production. *Endocrinology* **159**, 2815–2825 (2018).
56. W. Kuswanto *et al.*, Poor repair of skeletal muscle in aging mice reflects a defect in local, interleukin-33-dependent accumulation of regulatory T cells. *Immunity* **44**, 355–367 (2016).
57. D. Burzyn *et al.*, A special population of regulatory T cells potentiates muscle repair. *Cell* **155**, 1282–1295 (2013).
58. I. D. Vainchtein *et al.*, Astrocyte-derived interleukin-33 promotes microglial synapse engulfment and neural circuit development. *Science* **359**, 1269–1273 (2018).
59. W. Y. Chen, J. Hong, J. Gannon, R. Kakkar, R. T. Lee, Myocardial pressure overload induces systemic inflammation through endothelial cell IL-33. *Proc. Natl. Acad. Sci. U.S.A.* **112**, 7249–7254 (2015).
60. C. Moussion, N. Ortega, J.-P. Girard, The IL-1-like cytokine IL-33 is constitutively expressed in the nucleus of endothelial cells and epithelial cells in vivo: A novel 'alarmin'? *PLoS One* **3**, e3331 (2008).
61. M. Pichery *et al.*, Endogenous IL-33 is highly expressed in mouse epithelial barrier tissues, lymphoid organs, brain, embryos, and inflamed tissues: In situ analysis using a novel Il-33-LacZ gene trap reporter strain. *J. Immunol.* **188**, 3488–3495 (2012).
62. V. Topping *et al.*, Interleukin-33 in the human placenta. *J. Matern. Fetal Neonatal Med.* **26**, 327–338 (2013).

63. M. W. Dahlgren *et al.*, Adventitial stromal cells define group 2 innate lymphoid cell tissue niches. *Immunity* **50**, 707–722.e6 (2019).
64. A. A. Ashkar, J. P. Di Santo, B. A. Croy, Interferon gamma contributes to initiation of uterine vascular modification, decidual integrity, and uterine natural killer cell maturation during normal murine pregnancy. *J. Exp. Med.* **192**, 259–270 (2000).
65. K. Woidacki *et al.*, Mast cells rescue implantation defects caused by c-kit deficiency. *Cell Death Dis.* **4**, e462 (2013).
66. A. S. Care *et al.*, Reduction in regulatory T cells in early pregnancy causes uterine artery dysfunction in mice. *Hypertension* **72**, 177–187 (2018).
67. P. D. Lima, J. Zhang, C. Dunk, S. J. Lye, B. A. Croy, Leukocyte driven-decidual angiogenesis in early pregnancy. *Cell. Mol. Immunol.* **11**, 522–537 (2014).
68. Y. R. Sheng *et al.*, IL-33/ST2 axis affects the polarization and efferocytosis of decidual macrophages in early pregnancy. *Am. J. Reprod. Immunol.* **79**, e12836 (2018).
69. T. Stampalija *et al.*, Soluble ST2, a modulator of the inflammatory response, in preterm and term labor. *J. Matern. Fetal Neonatal Med.* **27**, 111–121 (2014).
70. L. M. Scott *et al.*, Production and regulation of interleukin-1 family cytokines at the materno-fetal interface. *Cytokine* **99**, 194–202 (2017).
71. J. Kieckbusch, L. M. Gaynor, F. Colucci, Assessment of maternal vascular remodeling during pregnancy in the mouse uterus. *J. Vis. Exp.* (106), e53534 (2015).
72. A. M. Beaulieu, N. Valero-Pacheco, IL-33+ cell subsets in the decidua and myometrium of pregnant mice at E7.5. Gene Expression Omnibus. https://www.ncbi.nlm.nih.gov/geo/query/acc.cgi?acc=GSE209795. Deposited 26 July 2022.
73. A. M. Beaulieu, N. Valero-Pacheco, Immune cell distribution in the decidua and myometrium of pregnant mice at E7.5). Gene Expression Omnibus. https://www.ncbi.nlm.nih.gov/geo/query/acc.cgi?acc=GSE209796. Deposited 26 July 2022.